Development of novel low-bandgap conjugated polymers for organic solar cells

Jianping Lu,[†,] Ta-Ya Chu,[†] Salem Wakim,[†] Yanguang Zhang,[†] Sai-Wing Tsang,[†] Jiayun Zhou,[†] Serge Beaupré,[‡] Mario Leclerc,[‡] and Ye Tao[†,*]*

Overwrite † Institute for Microstructural Sciences (IMS), National Research Council of Canada (NRC), Ottawa, ON, K1A 0R6, Canada, ‡ Département de Chimie, Université Laval, Quebec City, QC, Canada G1V 0A6

Introduction

Bulk heterojunction (BHJ) organic solar cells based on conjugated polymers and soluble fullerene derivatives have the potential to offer low-cost solar electricity by using spin-coating, ink-jet printing, or roll-to-roll printing techniques to fabricate large-area photovoltaic devices on flexible and light-weight substrates.[1] The power conversion efficiencies (PCE) of solution-processed polymer solar cells have reached 7-8% level primarily due to the development of new low-bandgap *p*-type materials and better control of the nano-scale morphology of the interpenetrating electron donor/acceptor networks.[2] The device structure of typical BHJ solar cells is as follows: A transparent conductive anode (e.g. ITO)/poly(3,4-ethylenedioxythiophene)-poly(styrene sulfonate) (PEDOT-PSS)/a BHJ active layer/a low work-function metal cathode (e.g. Ca and LiF/Al). However, there are several stability issues associated with this device structure, such as the rapid oxidation of the low work-function metal cathodes when exposed to air and water vapor, the slow etching of ITO by the acidic PEDOT-PSS, and the instability of the interface between the active layer and the cathode.[3] Therefore, encapsulation with high oxygen and water vapour barriers is required for the typical organic solar cells, leading to greatly increased production cost.

To overcome the above-mentioned problems, there is a growing interest in the development of inverted organic solar cells,[4] where an air-stable high work-function metal (e.g. Au and Ag) is used as the top anode to collect holes, transparent ITO is used as the bottom cathode to collect electrons, and air-stable metal oxides are used as interlayers between the active layer and the electrodes to help charge extraction. As such, the stability of the inverted solar cells has been significantly improved. In order to set the polarity of charge collection properly in an inverted solar cell, an n-type metal oxide such as titanium oxide (TiO_x), zinc oxide (ZnO) and cesium carbonate (Cs_2CO_3), is deposited on the ITO electrode to lower its work function, and a thin layer of MoOx is inserted between the active layer and the anode as a hole-selecting layer.

Recently, we reported a promising copolymer of 4,4-bis(2-ethylhexyl)-dithieno[3,2-b:2',3'-d]silole and *N*-octylthieno[3,4-c]pyrrole-4,6-dione (PDTSTPD),[5] which possesses both a low optical energy gap (1.73 eV) and a deep HOMO energy level (5.57 eV). A high V_{oc} (~0.9V) and a high J_{sc} (~12 mA/cm^2). In this work, we report air-stable inverted organic solar cells by using an annealing-free ZnO nanocrystal film as the electron transporting layer and a BHJ film consisting of PDTSTPD and $PC_{71}BM$ as the active layer.We demonstrated that the processing additives have significant impact on the device stability. By replacing the widely used 1,8-diiodooctane (DIO) with nitrobenzene as the processing additive, an EQE calibrated power conversion efficiency of 6.7% was achieved on the inverted solar cells with an active area of 1.0 cm^2. In addition, we also investigated the effect of the polymer molecular weight on the blend film morphology and OPV performance. A power conversion efficiency as high as 7.7% was achieved on regular solar cells with 1.0 cm^2 active area, which is among the best performance up to date.

Results and Discussion

2.1 Molecular weight effect

We prepared a series of PDTSTPD copolymers with number-average molecular weights of 10 KDa, 18 KDa, and 31 Kda, respectively. These three PDTSTPDs of different molecular weights were obtained by Soxhlet extraction using different solvents. The 10 KDa fraction was extracted by hot hexanes, the 18 KDa fraction by dichloromethane, and the 31 KDa part by chloroform. Therefore, these three polymers have very different solubility in organic solvents; the higher molecular weight polymer has lower solubility. The absorption spectra of PDTSTPDs of Mn = 18 KDa and 31 KDa are almost the same, indicating that the effective conjugation length for the optical bandgap of PDTSTPD is below 18 KDa. However, the low molecular weight fraction (10 KDa) has a slightly larger optical energy gap, with a 6 nm blue shift in the absorption spectrum as shown in Figure 1. A PCE of 3.1% was obtained with the low molecular weight PDTSTPD, which is similar to the result (2.13%) published by Zhang *et al.* from the same polymer with a molecular weight of 13.6 KDa.[6] Significant improvement in PV performance was observed with high molecular weight PDTSTPDs, as shown in Figure 2. The PCE was improved to 5.4% and 7.7% when the molecular weight increased to 18 KDa and 31 KDa, respectively. There is less than 4% deviation in J_{sc} between the solar simulator and EQE measurements. The EQE spectra of the OPV devices made from PDTSTPDs of different molecular weights show significant improvement across the whole photo response region with increasing polymer molecular weight. The hole mobility of PDTSTPD increased from $7x10^{-6}$ to $1x10^{-4}$ and $3.7x10^{-4}$ cm^2/Vs, when the molecular weight increased from 10 KDa to 18 KDa and 31 KDa. The OPV cells made with high molecular weight PDTSTPD not only had a higher J_{sc}, but also exhibited a higher fill factor (FF). The enhanced FF is attributed to a relatively low series resistance of the cell due to the high hole mobility of the high molecular weight PDTSTPD. The series resistance of OPV cells decreased from 9 to 5 Ω cm^2 when the molecular weight of the polymer increased from 10 KDa to 31 KDa. In addition, the enhanced OPV performance is not only due to the increased carrier mobility, but also due to the improved nano-scale morphology of the BHJ film. As compared with the change in hole mobility between 18 KDa and 31 KDa polymers, the improvement in PCE is much more significant (more than 40%). The improvement in mobility alone cannot fully explain the ~40% gain in PCE. Through atomic force microscopy (AFM) study, we can reasonably attribute the PCE gain partly to the improved nano-scale morphology of the interpenetrating PDTSTPD/ $PC_{71}BM$ network with increasing polymer molecular weight. The blend film prepared with low molecular weight (10 KDa) PDTSTPD and $PC_{71}BM$ shows a clear phase-separated morphology with finer fibrous nanoscale domains. When the polymer molecular weight increases, its solubility decreases and it tends to form aggregates. As a result, the domain size becomes larger and meanwhile less discontinuous phase separation is observed. From the above observation, we conclude that the polymer molecular weight significantly influences the PV performance via their impact on both the active layer morphology and charge mobility.

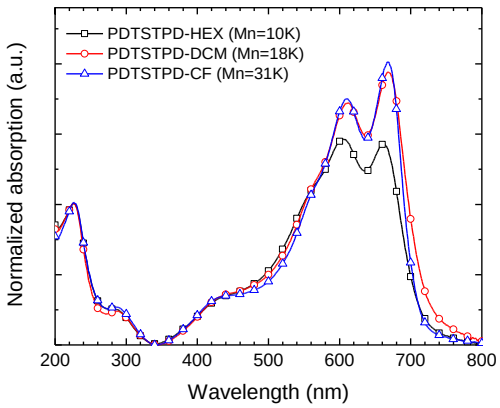

Figure 1. Absorption spectra of the different molecular weight PDTSTPDs.

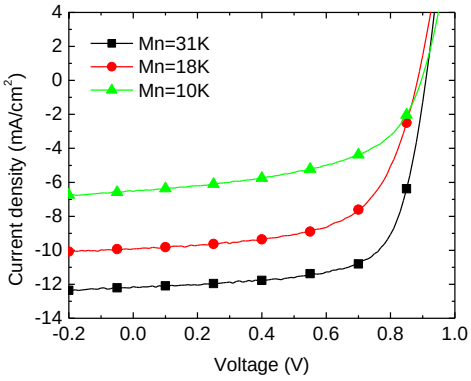

Figure 2. Current density-voltage characteristics of the solar cells fabricated with different molecular weight PDTSTPDs blended with $PC_{71}BM$ under AM 1.5G illumination.

2.2 Inverted solar cells

The active layer consisting of PDTSTPD and $PC_{71}BM$ (1 :2 by weight) was spin-cast on top of the ZnO film from a chlorobenzene solution containing 3 vol% DIO or 4 vol% nitrobenzene. The active layer thickness was controlled at 90 nm. Then, MoO_x and Ag were sequentially vacuum-deposited as the hole-extracting layer and the anode, respectively. The solar cells were then tested in air without encapsulation under AM 1.5G irradiation of 100 mW/cm^2. Under simulated 1-sun irradiation, the DIO devices gave an open-circuit voltage (V_{oc}) of 0.88 V, a short-circuit currnt (J_{sc}) of 11.1 mA/cm^2, and a remarkably high fill factor (*FF*) of 0.71. The overall power conversion efficiency reached 6.6% (using the J_{sc} calculated from the EQE measurement). For the nitrobenzene device, the EQE-calibrated J_{sc} is increased to 11.3 mA/cm^2, and the overall power conversion efficiency reaches 6.7% with a V_{oc} of 0.886 V and a *FF* of 67%. More importantly, this nitrobenzene device is remarkably stable with no degradation in the first two days in air. As can be seen from Figure 3, the non-encapsulated device retains 85% of its original efficiency even after exposed to the air for 32 days. The reason why the nitrobenzene device is more stable than the DIO device is under investigation.

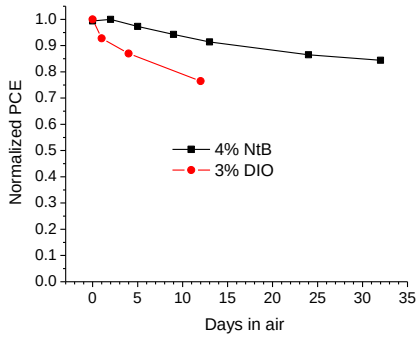

Figure 3. Normalized PCEs of the non-encapsulated inverted solar cells as a function of storage time in air.

Conclusions

In summary, we have demonstrated high-efficiency inverted BHJ solar cells with greatly improved air stability by using annealing-free ZnO nanocrystals as an electron-transporting layer and nitrobenzene (4 % by volume) as a processing additive for the PDTSTPD/$PC_{71}BM$ system. In addition, we have investigated the effect of the polymer molecular weight on the photovoltaic performance. High molecular weight PDTSTPD is required for photovoltaic application because of the associated high mobility in the polymer. The fill factor has been increased to 70% due to the decreased series resistance when using high molecular weight PDTSTPD (31 KDa) in both regular and inverted solar cells.

Acknowledgement. The financial support from Sustainable Development Technology Canada (SDTC) is greatly acknowledged.

References

(1) (a) Gunes, S.; Neugebauer, H.; Sariciftci, N. S. *Chem. Rev.* **2007,** *107*, 1324-1338. (b) Krebs, F. C. *Sol. Energy Mater. Sol. Cells* **2009**, *93*, 394-412. (c) Krebs, F. C. *Sol. Energy Mater. Sol. Cells* **2009**, *93*, 465-475. (d) Hoppe, H.; Sariciftci, N. S. *J. Mater. Chem.* **2006**, *16*, 45-61. (e) Dennler, G.; Scharber, M. C.; Brabec, C. J. *Adv. Mater.* **2009**, *21*, 1323-1338. (f) Brabec, C. J.; Gowrisanker, S.; Halls, J. J. M.; Laird, D.; Jia, S.; Williams, S. P. *Adv. Mater.* **2010**, *22*, 3839-3856.

(2) (a) Liang,Y.; Xu, Z.; Xia, J.; Tsai, S.; Wu, Y.; Li, G.; Ray, C.; Yu, L. *Adv. Mater.* **2010**, *22*, E135-E138. (b) Chen, H. Y.; Hou, J.; Zhang, S.; Liang, Y.; Yang, G.; Yang, Y.; Yu, L.; Wu, Y.; Li, G. *Nature Photon.* **2009**, *3*, 649-653. (c) He, Z.; Zhong, C.; Huang, X.; Wong, W.; Wu, H.; Chen, L.; Su, S.; Cao, Y. *Adv. Mater.* **2011**, 23, 4636.

(3) de Jong, M. P.; van IJzendoorn, L. J.; de Voigt, M.J.A. *Appl. Phys. Lett.* **2000**, *77*, 2255-2257.

(4) (a) White, M. S.; Olson, D. C.; Shaheen, S. E.; Kopidakis, N.; Ginley, D.S. *Appl. Phys. Lett.* **2006**, *89*, 143517. (b) Hau, S. K.; Yip, H. L. Baek, N. S.; Zou, J.; O'Malley, K.; Jen, A.K.Y. *Appl. Phys. Lett.* **2008**, *92,* 253301.

(5) Chu, T.-Y.; Lu, J.; Beaupré, S.; Zhang, Y.; Pouliot, J.-R.; Wakim, S.; Zhou, J.; Leclerc, M.; Li, Z.; Ding, J.; Tao, Y. *J. Am. Chem. Soc.* **2011**, *133*, 4250;

(6) Zhang, Y.; Zou, J.; Yip, H.-L.; Sun, Y.; Davie, J. A.; Chen, K.-S.; Acton, O.; Jen, A. K.-Y. *J. Mater. Chem.* **2011**, *21*, 3895